

Effect of fan arrangement and air flow direction on thermal performance of radiators in a power transformer

Sachin. B. Paramane^{a,*}, Wim Van der Veken^b, Atul Sharma^c, Joris Coddé^d

^aGlobal R&D Centre, Crompton Greaves Ltd., Mumbai, 400042, India;

^bCrompton Greaves Power Systems Belgium NV, Antwerpsesteenweg 167, 2800 Mechelen, Belgium;

^cIndian Institute of Technology Bombay, Mumbai, 400076, India;

^dUniversity of Leuven, Division of Applied Mechanics and Energy Conversion (TME), Celestijnenlaan 300-box 2421, 3001 Leuven, Belgium;

Abstract

The focus of the present numerical work is to study the effect of fan air flow direction and mounting arrangement on the thermal performance of the radiators of power transformers using Computational Fluid Dynamics analysis. The study is carried out for four radiators of 3 m height and 30 fins with 0.52 m width and two fans of 1 m diameter in vertical and horizontal air flow directions. The horizontal flows from the two fans are considered in the same and the opposite direction, with the fans located on the same and the opposite side, respectively running at the same speed of 860 rpm for all configurations. Thermal radiation is modelled using the discrete transfer radiation model. A comparison of different flow and heat transfer patterns as well as heat dissipation—for the four different configurations—is presented. Velocity and temperature contours are used to visualize the heat and fluid flow distribution over the radiators. Fans placed on one side of the radiators result in larger heat dissipation than the other arrangements studied. The reasons for the improvement in heat dissipation are presented.

Keywords: radiators; fan arrangement; cross flow; heat dissipation; CFD; flow distribution; transformer cooling

1. Introduction

Power transformers are expensive and critical components in the electricity network. Therefore it is important for network operators that the transformers work reliably over their expected lifetime to provide continuous power supply. Thus thermal management of these pieces of equipment is of great importance and the cooling system plays a vital role. Most of the published literature is on internal cooling of the power transformer, i.e., cooling of windings.

Transformer manufacturers are keen to reduce the number of radiators and fans—in order to reduce the weight of the system—without compromising on the thermal performance. With the advent of advanced tools like CFD (Computational Fluid Dynamics), nowadays it is possible to visualize virtually the air flow and temperature distribution over the radiators, thereby avoiding expensive experiments. This visualization of air flow distribution gives insight for improving the thermal performance of the system by identifying the region of lower and higher air flow and recirculation regions.

In the past very limited experimental and numerical work related to power transformer radiator cooling performance was reported. In their study the authors of [1] described a numerical simulation for improving heat transfer in a power transformer, with the help of the thermal head (difference in elevation between the center of the coils and the center of the radiators). They mentioned that by increasing the thermal head there can be a saving of the heat transfer area of the radiators if the mass flow of oil is increased. CFD analysis to determine temperature distribution and flow pattern in a block radiator used in power transformer cooling system was carried out by [2]. They mainly focused on studying the relation between radiator block characteristics and the cooling behavior of the system. Optimum designs of an ONAN (Oil Natural Air Natural) transformer cooling system by using advanced numerical thermal field and computational fluid dynamics techniques was done by [3]. They examined novel tank designs in conjunction with other crucial parameters, such as the number and location of the winding cooling ducts, so as to define the best optimum geometry that ensures maximum efficiency performance of the transformer cooling system. They observed that curved panel surfaces deliver better thermal performance since they enhance dynamic oil circulation characteristics. Authors of [4]

*Corresponding author

Email address: sachin.paramane@cgglobal.com (Sachin. B. Paramane)

studied the heat transfer in large air cooled radiators using a CFD model in which the mixed convection based oil/air flow and the heat transfer in the radiators is modelled using an anisotropic porous medium approach; and the area surrounding the radiators using a standard turbulent heat transfer model. The thermal behavior of several ONAN distribution transformers are modelled by [5]. A computationally efficient model to represent the thermal performance of an ONAN distribution transformer located in open air conditions was developed and numerically solved using CFD techniques. They evaluated the influence of turbulence modelling on the model's predictions. A network model for the buoyancy driven flows of oil and air in radiators used for cooling of power transformers by considering the entire oil flow circuit of a power transformer was presented by [6]. The radiators are treated as counter flow heat exchangers and analytical expressions are used for the temperature distributions in oil and air. It was observed that for operating conditions normally found for mineral oil, the counter flow assumptions for heat flux distribution gives approximately the same results as if uniform heat flux was assumed. Authors of [7] presented an analytical, numerical and experimental study on the cooling performance of radiators—used in oil filled power transformer applications—with non-direct flow (ONAN) and direct-oil-forced flow (ODAN). They predicted radiator temperature distribution and cooling performance analytically, which was validated with their CFD results. CFD analysis for the effect of air flow direction and fan offset on ONAF (Oil Natural Air Forced) cooling performance of a 25 MVA transformer is presented by [8]. They proposed a factor of merit to compare the thermal performance of different thermal systems of transformer. However, quantitative analysis for improvement in the heat dissipation was not discussed in detail. Recently, the development of a thermohydraulic radiator model based on physical equations for accurate prediction of oil temperatures is described by [9]. For the thermal calculations a method was developed to predict air velocity as a function of fan characteristics and radiator geometry.

Fan-configurations in a power transformer—commonly used by various manufacturers—are of two types: horizontal and vertical; mounted at the sides or at the bottom of the radiator assembly, respectively. Furthermore for horizontal air flow, fans can be placed at the top, opposite to each other, and in a staggered arrangement. Transformer manufacturers are keen to determine which is the better fan mounting arrangement of these configurations. However, there is no published literature on comparing these four fan mounting arrangements. The major objective of the present work is to study the thermal performance of the radiator in a power transformer, under the effect of different fan mounting arrangements, using Computational Fluid Dynamics analysis.

2. Physical Description of the Problem

Fig. 1 shows the front view of the four different radiator-fan configurations, considered in the present study; using Ansys CFX commercial Computational Fluid Dynamics anal-

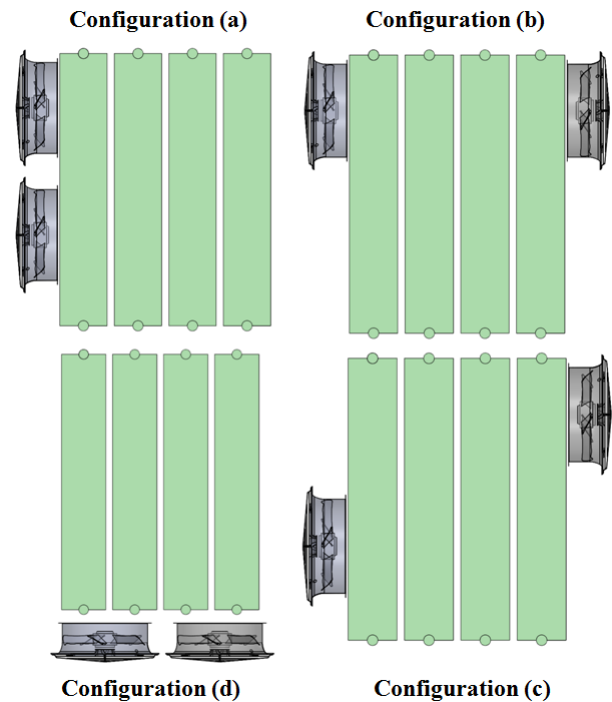


Figure 1: Schematic diagram of four different mounting arrangements of two fans in the four radiator assembly: (a) one-sided mounted fans (b) opposite-side mounted fans at the top (c) opposite-side mounted fan with one at the top and the other at the bottom and (d) bottom mounted fans

ysis software. The figure shows four radiators, with each of them consisting of 30 fins (steel + oil channel) of 3 m height, 0.52 m width and 0.0085 m thickness. The fins are seen in Fig. 2a which is horizontally spaced with a gap of 50 mm and two fans (of 1 m diameter, having 7 blades rotating at a speed of 860 rpm) are mounted in different positions (Fig. 1). The configurations correspond to the radiator assembly, with (a) one-sided mounted fans (b) opposite-side mounted fans at the top (c) opposite-side mounted fans with one at the top and the other at the bottom and (d) bottom mounted fans. The direction of fan induced flow is horizontal for the first three configurations and vertical for the fourth configuration. The radiators are steel plate heat exchangers, installed vertically next to the transformer. They consist of a number of panels, made up of two steel plates which are pressed and welded on each other. A passage for the flow of oil is formed in the radiator—by creating channels between the steel plates of the panels. As the oil flows through these channels, heat is transferred from the oil to the steel plate and further to the air flowing between the radiator panels. Finally, the oil flowing downwards in the radiator panels enters into the bottom header pipe and reaches back to the transformer tank.

3. Numerical Methodology

Commercial CFD software (Ansys CFX Version 12.1) is used in the present work. Governing equations, computational

domain, boundary conditions, grid generation and solution methodology are presented below.

3.1. Governing Equations

The steady Navier-Stokes (NS) equations for an incompressible fluid are considered as:

$$\frac{\partial u_i}{\partial x_i} = 0 \quad (1)$$

$$u_i \frac{\partial u_j}{\partial x_i} = \frac{\partial}{\partial x_j} \left[(\nu + \nu_t) \frac{\partial u_j}{\partial x_i} \right] - \frac{\partial p}{\partial x_j} \quad (2)$$

where u_i are the mean velocity components, p is the pressure, and ν and ν_t the laminar and turbulent viscosity, respectively. Additional equations for turbulent quantities are considered to compute the eddy viscosity and are given in [10].

3.2. Computational Domain

In the present work, a domain independence study is carried out and a computational domain which is sufficiently far away from the geometry is considered for the analysis. Fig. 2a shows the present computational domain, consisting of two boundaries: inner and outer. There are six outer boundaries which surround the radiator-fan configuration. Since the radiators are not mounted on the transformer tank, all the boundaries are open boundaries except ground, which has a wall boundary condition. It is ensured that there is no appreciable change in the results, with further increase in the distance of the open boundaries (shown in the figure) from the radiator-fan assembly.

3.3. Grid Generation

Since the geometry in the present study is highly skewed due to its varied dimensions (especially for radiator plates, with height of 3 m and thickness of the plates is 1 mm), the geometry is simplified so that there is a negligible effect on the results for the actual system. Geometry clean-up is done in Solidworks software by removing the brackets, lifting lug and other small parts; which will not have any significant effect on flow and heat transfer. This also helped reduce the time required for meshing.

Hybrid mesh (hexahedral and tetrahedral) is used in the present study for solving the governing equations. Hexahedral elements are used for the radiators for resolving detailed flow features, better convergence and accuracy. Tetrahedral elements are used for meshing of the fans and rotating domain, due to the complexity of the fan blade profile. Both these domains are merged by defining a suitable interface at the merging surface. Mesh generation is done using commercial mesh generation Ansys ICEM CFD software. Mesh quality—for the various regions in the domain—is controlled by using different options in the software. In order to locate the first grid point target y^+ value of 20 is considered and first cell height is calculated as 1 mm. Thus, during the mesh generation, the first cell height is 1 mm from the wall of the radiator plates. This turned out to be effective for

the mesh independence study. 7.7 million nodes were found to be a sufficient number for grid-independent results. The mesh on a plane passing through the fan center is shown in Fig. 2b—a close up view near the fan and the radiator is shown in Fig. 2c.

3.4. Boundary Conditions

Boundary conditions play an important role in CFD simulations and dictate the solutions. In the present analysis, air at an ambient temperature of 39.8°C is chosen as a working fluid. It corresponds to a typical high ambient temperature in the summer season of a tropical country like India. Side walls are considered as opening boundaries, whereas the ground as a no-slip wall. A very low intensity of turbulence (1%) is specified for an opening boundary condition.

The heat and fluid flow for a radiator-fan configuration is a combined internal and external flow: internal oil-flow in the channels of the radiator panels and external air-flow over radiator. The internal flow simulation is avoided, to reduce the computational complexity of the present problem without significantly compromising the accuracy of the results. This is done by approximating the temperature variation on the surface of the radiator as linear [2], with a temperature of 56.1°C at the top and 42.9°C at bottom of the radiator panel. No-slip BC is used on the surface of radiator plates and fans. Moreover, this simplification can be allowed here, since we are mainly focused on comparing the efficiency of different air flow directions. This efficiency difference will be mainly determined by differences in the air domain. The rotation of the fan at a specified speed—which significantly impacts the air flow distribution over the radiators—is indeed considered in the present work. A rotating frame of reference (RFR) is used for modelling the rotating fan, with a fluid sub-domain (surrounding the fan) rotating at an angular velocity corresponding to that of the fan. A frozen rotor interface is applied between stationary and rotating domain to connect these domains with a general connection. Other than the radiator plates, all other no-slip walls are approximated as adiabatic.

The Discrete Transfer Model (DTM) [10] is applied to model the surface radiation heat transfer in the present study. The main assumption of the DTM is that the radiation leaving the surface element in a certain range of solid angles can be approximated by a single ray. There are four methods for calculation of heat propagation by radiation (Rosseland Model, P1 Model, Discrete Transfer Model and Monte Carlo Model) in [10]. The radiation is represented by particles which are tracked through the air domain using a Ray-tracing method [11]. The spectral radiative transport equation used in [10, 11] is:

$$\frac{dI_v(\vec{r}, \vec{s})}{ds} = -(K_{av} + K_{sv}) \cdot I_v(\vec{r}, \vec{s}) + K_{av} \cdot I_b(v, T) + \frac{K_{sv}}{4\pi} \int dI_v(\vec{r}, \vec{s}') \cdot \Phi \cdot (\vec{s} \cdot \vec{s}') \cdot d\Omega + S \quad (3)$$

where: I_b —blackbody emission intensity, W/m^2 ; I_v —spectral emission intensity, W/m^2 ; \vec{r} —position vector, m; \vec{s} —direction vector, m; s —path length, m; K_a —absorption

coefficient; K_s —scattering coefficient; V —frequency, s^{-1} ; T —local absolute temperature, K; Φ —in-scattering phase function, Ω —solid angle, rad; S —a source term, W/m^2 .

3.5. Solution Methodology

The governing equations solved for the present problem consist of incompressible Navier-Stokes equation. Although the medium is a compressible fluid (air) the incompressible Navier-Stokes equations are allowed due to the low Mach number of the flows. The Reynolds number calculated for case (d) is of the order of 41720 hence flow is turbulent and the Shear Stress Transport (SST) model is used here for modelling turbulence, as it has been found to be better for external flows, both in our previous study as well as the published literature. Furthermore, as the velocities in the present problem are not very high (in the order of 6.6 m/s), the thermal instead of the total energy model is used for heat transfer. It should be noted that the influence of viscous dissipation is neglected as the working fluid is Newtonian and there is no appreciable change in viscosity for the range of temperature found here. Radiation is modelled in the present study for all the cases.

The commercial flow solver Ansys CFX is used and simulations are done on a workstation, with a clock speed of 3.33 GHz and 64 GB RAM. Computation time required for completing one simulation on eight parallel processors is approximately 25 hrs. Convergence is achieved by ensuring that root mean square (rms) residuals are below 10^{-4} and imbalance within the domain is less than 1%. Excellent agreement of the present computational methodology with the present experimental results for mass flow rate (from fan) and heat dissipation (from radiator in ONAN and ONAF configuration) was presented in our recent work [8] and the code validation is not shown here.

4. Results And Discussions

This section starts with the qualitative results to explore the velocity/temperature distribution, heat flux distribution on radiators etc. Thereafter, quantitative results are discussed in a separate subsection for heat flux and heat dissipation from the radiators below.

4.1. Heat and fluid flow patterns

Fig. 3 shows the vectors and Fig. 4 shows the contours of velocity at a central plane passing through the fans for all four configurations. For configuration (a), Fig. 3a shows that the air enters both the fans mainly from the left and top/bottom side and passes over the radiator. Fig. 4a shows that the footprint of the AF cooled area increases somewhat from the first to the last radiator. However, with increasing footprint there is also a significant reduction in air speed. For configuration (b), Fig. 3b shows that the air enters from the left, right and top/bottom and is thrown over the radiators opposite to each other. It can be seen that the air streams from left and right strike each other and part of the air moves towards

the top whereas part of the air moves towards the bottom, touches the ground and escapes towards the left and right. Placing the fans opposite each other creates a large counter pressure on each fan. This pushes the air flow outside (to the top and bottom) creating a large leakage of air flow and vertical (top to bottom) air flow in the middle radiators of the radiator group, shown in Fig. 4b. Since this situation is symmetric, it can be represented as if there were be a wall in the middle of the radiator group. For configuration (c), Fig. 3c and 4c shows that the left fan covers the bottom part of the radiator whereas the right fan covers the top portion of the radiators. Air streams from both fans strike at the center of the radiators and get slightly inclined towards the bottom and the top for the left and right fan, respectively.

For vertical blowing in configuration (d), Fig. 3d and 4d shows that the air enters from the bottom, left and right side and is thrown over the radiators towards the top. The figures also show that part of the air escapes from the left and right sides of the top region. Furthermore, it can be observed that the velocity is lower just above the hub portion of the fan and also in between the two fans. A similar air flow pattern was observed in our earlier publication for vertical air flow configuration [8].

Fig. 5 show the temperature contours at the central plane for all configurations. A correlation between the air speed contours can be observed for all configurations. For horizontal air flow, hot air exits mostly from the top portion of the last radiator as shown in Fig. 5a. Furthermore, Fig. 5b, shows that hot air streams from the two fans strike at the center and move towards the ground and escape from left and right. Hence there are higher temperature contours compared to other figures. Moreover, Fig. 5c shows that there is some recirculation of hot air. Part of the hot air exiting the radiator assembly enters the opposite fan, resulting in slightly higher entrance temperature. For vertical air flow, Fig. 5d shows the air heating up between the radiator panels. In the area between the radiator panels with low air speed (above the collector), the air heats up most. Air is heated up further and mixed when moving upwards and hot air escapes the radiators from the sides and top.

4.2. Velocity Contours

Fig. 6 show the velocity contours for all the configurations at two horizontal planes along the height of radiators. Fig. 6a shows that there is a steadily decreasing air flow towards the last radiators. The footprint of the higher velocity air is clearly visible for the first radiator. Fig. 6b shows the two air streams striking each other and larger regions of the radiators are unutilized for heat dissipation. Due to the air pushing opposite to each other, the figure shows that the first and fourth radiators are less utilized for heat dissipation than the 2nd and 3rd radiators. Fig. 6c shows that due to air pushing opposite to each other the velocity drops from the 2nd to the 3rd radiator. It can be seen from Fig. 6d that there is a footprint of higher velocity air at the bottom.

Furthermore, the figure shows that the flow is restricted within the radiator assembly in the bottom plane. However,

as the fluid flows upward, it goes in between the plates and starts escaping from the sides in the middle and top plane [8]. This can be attributed to two reasons. First, the air speed exiting the fan has a significant rotational component—caused by the rotation of the fan blade. When the air moves in between the radiator panels, only the component of the velocity parallel with the radiator plate remains. This velocity component moves the air in a parallel direction to the radiator panels, creating quadrants of higher and lower air speed. The second reason is the redistribution of the air speed. The air particles at the edge of the air cone are dragged forward by the air stream, resulting in a wider cone but with lower average air velocity.

4.3. Quantitative Heat Transfer Results

Fig. 7 shows the contours of the heat transfer coefficient over the surface of the radiator assembly. The figure shows a red colored footprint of higher heat transfer coefficient at the surface of the radiators for the horizontal as well as the vertical air flow. As expected, the areas of larger heat transfer match the areas with larger air velocity. Similar heat transfer coefficient distribution was observed for both cases in [8]. For configuration (a), although higher velocity of air is prevalent at both the top as well as the bottom, it can be observed from Fig. 7a that the heat transfer coefficient is larger at the top than the bottom of the radiator. This is due to the higher temperature of the radiator at the top than the bottom. Fig. 7d shows the footprint of the larger heat transfer coefficient in the vertical direction due to the increase in oil temperature towards the top of the radiator. However, this increase in the heat transfer coefficient is less than for example in case a, since situation (d) is in principle a counter flow heat exchanger. The effect of the higher flux due to the higher oil temperature is partially compensated by the increase in air temperature and the decrease in air velocity towards the top.

Fig. 8 I and II show the average heat transfer coefficient and total heat transfer rate for all configurations, respectively. It can be seen from Fig. 8 I that for configuration (a) there is a marginal increase in average heat transfer coefficient compared to configuration (d). However for configurations (b) and (c) the average heat transfer coefficient is lower than configurations (a) and (d). A similar trend can be seen for total heat dissipation from the radiators in Fig. 8 II. There is 1.4% more heat dissipation for configuration (a) than (d). However, the reduction in heat dissipation for configurations (b) and (c) is 3.4% and 8.5%, respectively. Thus all the above results show that configurations (a) and (d) have a significantly higher efficiency than configurations (b) and (c). Fans placed opposite to each other have a negative impact on heat dissipation.

5. Conclusions

CFD simulations were performed to study the heat transfer efficiency for four different fan mounting arrangements: horizontal flow for (a)–(c) and vertical flow for (d). The horizontal

flow from both fans is in the same direction for (a) and the opposite direction for (b) and (c). These analyses are done by assuming the same linear temperature profile for all four radiators (imposed boundary condition), while neglecting the tank wall adjacent to the radiator and the oil flow inside the radiator panels.

Configurations (a) and (d) result in almost the same heat dissipation. In both cases, the same panel temperature profile was imposed on the radiators, while in practice this can differ a little due to differences in oil temperature distribution over the panel. Configurations (b) and (c) result in lower heat transfer rates. Thus, it may be concluded that placing fans opposite each other has a negative impact on heat transfer dissipation.

Acknowledgments

The authors would like to acknowledge Global R&D Centre, Crompton Greaves Ltd. Mumbai, India for providing the computational resources and permission for publishing this work.

References

- [1] C.-H. Cha, J.-K. Kim, K.-Y. Kweon, Investigation of the thermal head effect in a power transformer, in: *Transmission & Distribution Conference & Exposition: Asia and Pacific*, 2009, IEEE, 2009, pp. 1–4.
- [2] H. Nabati, J. Mahmoudi, A. Ehteram, Heat transfer and fluid flow analysis of power transformer's cooling system using cfd approach, *Chemical Product and Process Modeling* 4 (1) (2009) 1934–2659.
- [3] E. I. Amoiralis, P. S. Georgilakis, M. A. Tsili, A. G. Kladas, Global transformer optimization method using evolutionary design and numerical field computation, *Magnetics*, IEEE Transactions on 45 (3) (2009) 1720–1723.
- [4] R. B. Fdhila, E. Kranenborg, T. Laneryd, C.-O. Olsson, B. Samuelsson, A. Gustafsson, L. Lundin, Thermal modeling of power transformer radiators using a porous medium based cfd approach, in: *Second International Conference on Computational Methods for Thermal Problems*, Dalian, China, 2011.
- [5] J. Gastelurrutia, J. C. Ramos, G. S. Larraona, A. Rivas, J. Izagirre, L. Del Río, Numerical modelling of natural convection of oil inside distribution transformers, *Applied Thermal Engineering* 31 (4) (2011) 493–505.
- [6] C. Olsson, Buoyancy driven flow in counter flow heat exchangers, in: *6th European Thermal Sciences Conference*, Poitiers, France, 2012, pp. 1–8.
- [7] M.-g. Kim, S. M. Cho, J.-K. Kim, Prediction and evaluation of the cooling performance of radiators used in oil-filled power transformer applications with non-direct and direct-oil-forced flow, *Experimental Thermal and Fluid Science* 44 (2013) 392–397.
- [8] S. B. Paramane, K. Joshi, W. Van der Veken, A. Sharma, Cfd study on thermal performance of radiators in a power transformer: Effect of blowing direction and offset of fans, *Power Delivery*, IEEE Transactions on 29 (6) (2014) 2596–2604.
- [9] W. Van der Veken, S. Paramane, R. Mertens, V. Chandak, J. Codde, Increased efficiency of thermal calculations via the development of a full thermohydraulic radiator model, *IEEE Transactions on Power Delivery* Accepted for publication.
- [10] ANSYS 2009. CFX manual. Theory. Version 12.1.
- [11] T. Zitzmann, P. Pfrommer, M. Cook, Dynamic thermal building analysis with cfd—modelling radiation, *Proceedings: Building Simulation*, Beijing, China (2007) 31–38.

Nomenclature

ODAN oil directed air natural

ONAF oil natural air forced

ONAN oil natural air natural

c_p Specific heat, J/(Kg·K)

k thermal conductivity of fluid, W/(m·K)

p pressure, N/m²

T Temperature, K

u velocity, m/s

x coordinate, m

ν kinematic viscosity of the fluid, m²/s

ρ density of the fluid, kg/m³

τ shear stress, N/m²

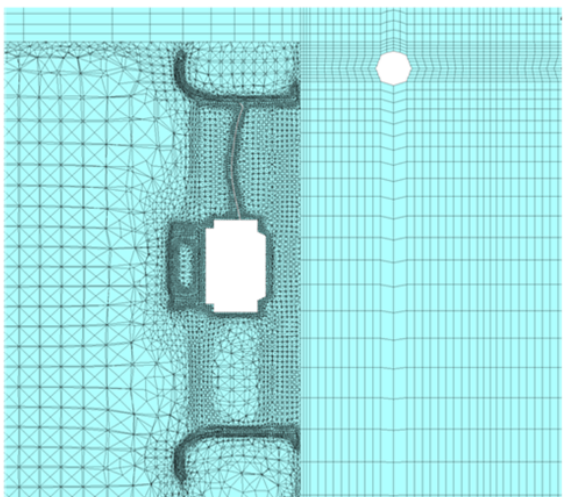
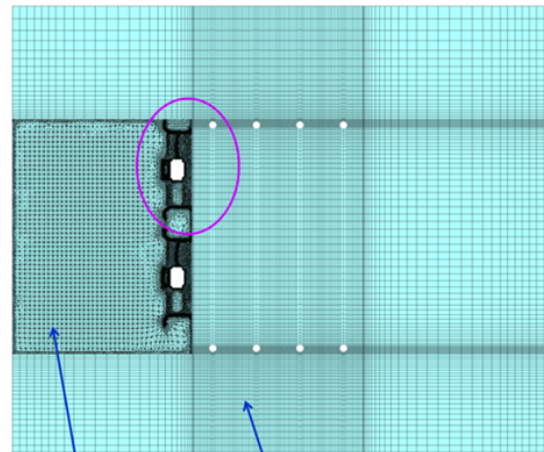
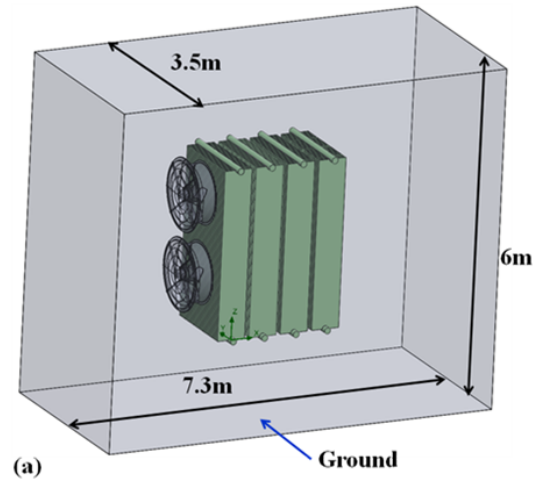


Figure 2: (a) Computational domain (b) Hybrid mesh used in the present study (c) close up view of mesh near fan and radiator

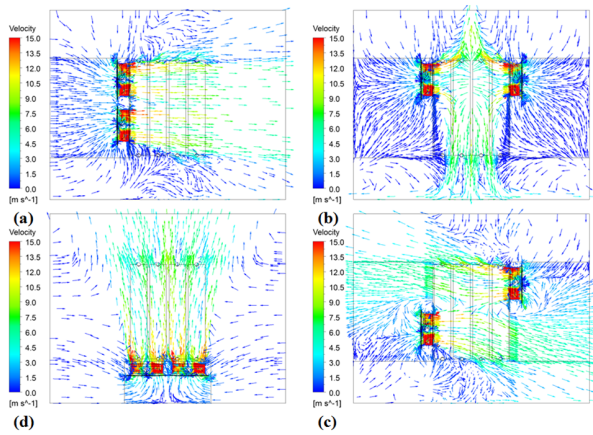


Figure 3: Velocity vectors in a plane passing through fan centers for the four configurations

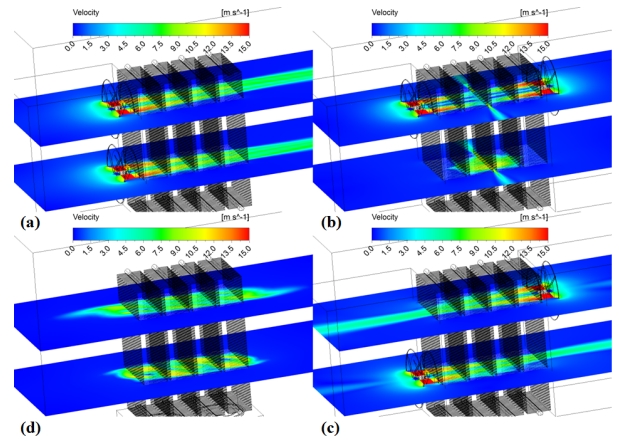


Figure 6: Velocity contours at two horizontal planes along the height of radiators, for the four configurations

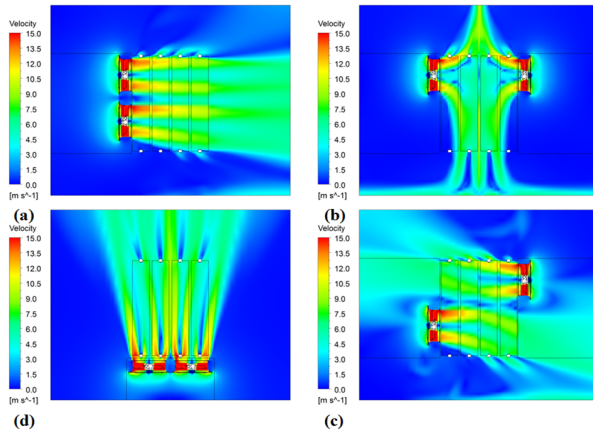


Figure 4: Velocity contours in a plane passing through fan centers for the four configurations

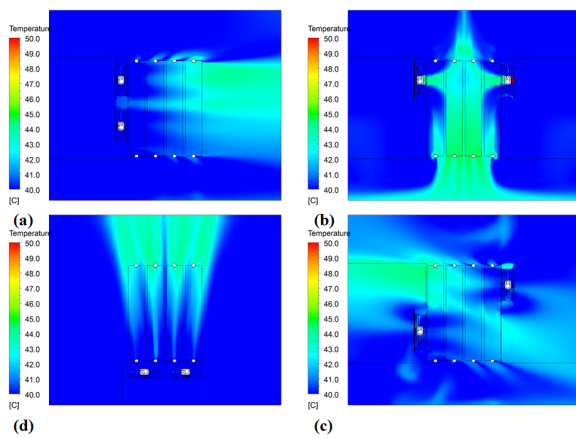


Figure 5: Temperature contours in a plane passing through fan centers for the four configurations

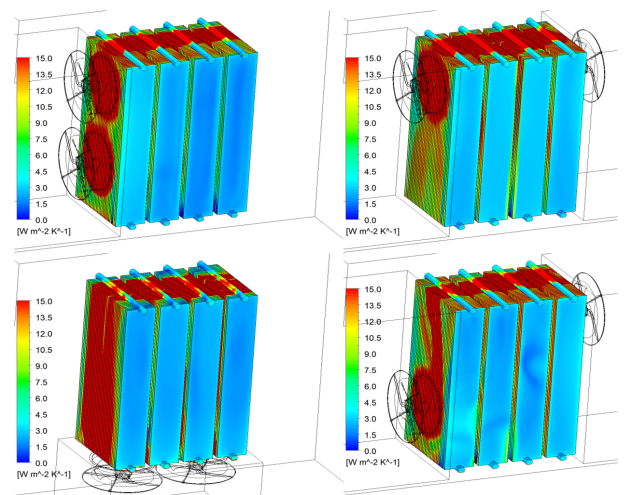


Figure 7: Heat transfer coefficient variation over the radiator surface

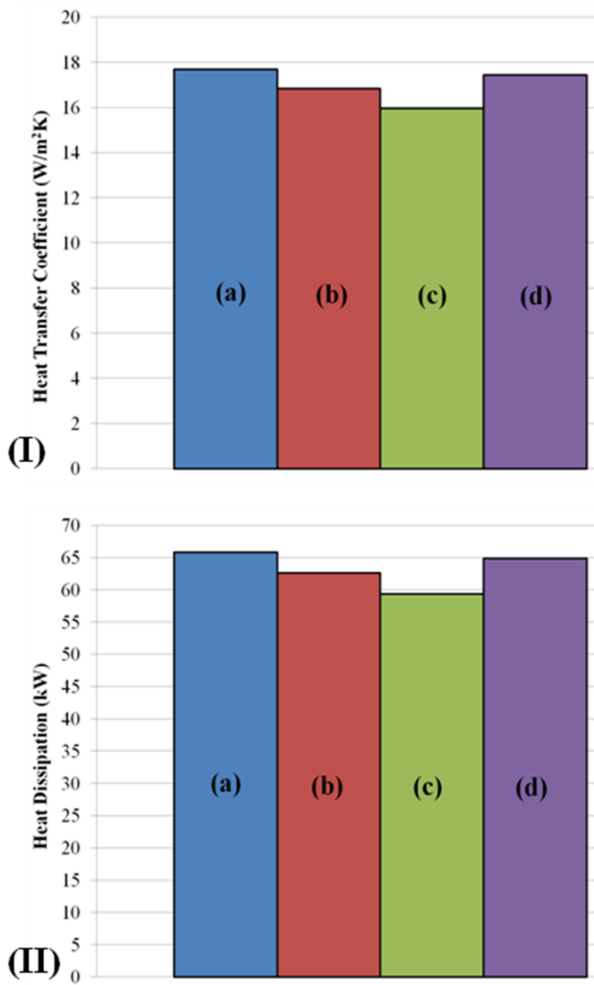


Figure 8: (I) average heat transfer coefficient and (II) total heat transfer rate for all configurations